Combustion and Flame 235 (2022) 111684

Contents lists available at ScienceDirect

Combustion and Flame

journal homepage: www.elsevier.com/locate/combustflame

Skeletal model reduction with forced optimally time dependent modes☆

A.G. Nouri[a,*], H. Babaee[a], P. Givi[a], H.K. Chelliah[b], D. Livescu[c]

[a] Department of Mechanical Engineering and Materials Science, University of Pittsburgh, Pittsburgh, PA 15261, USA
[b] Department of Mechanical and Aerospace Engineering, University of Virginia, Charlottesville, VA 22904, USA
[c] Los Alamos National Laboratory, Los Alamos, NM 87544, USA

ARTICLE INFO

Article history:
Received 1 March 2021
Revised 9 August 2021
Accepted 9 August 2021
Available online 30 August 2021

Keywords:
Model reduction
Skeletal model
Sensitivity analysis
Optimally time-dependent modes

ABSTRACT

Skeletal model reduction based on local sensitivity analysis of time dependent systems is presented in which sensitivities are modeled by forced optimally time dependent (f-OTD) modes. The f-OTD factorizes the sensitivity coefficient matrix into a compressed format as the product of two skinny matrices, *i.e.* f-OTD modes and f-OTD coefficients. The modes create a low-dimensional, time dependent, orthonormal basis which capture the directions of the phase space associated with most dominant sensitivities. These directions highlight the instantaneous active species, and reaction paths. Evolution equations for the f-OTD modes and coefficients are derived, and the implementation of f-OTD for skeletal reduction is described. For demonstration, skeletal reduction is conducted of the constant pressure ethylene-air burning in a zero-dimensional reactor, and new reduced models are generated. The laminar flame speed, the ignition delay, and the extinction curve as predicted by the models are compared against some existing skeletal models in literature for the same detailed model. The results demonstrate the capability of f-OTD to eliminate unimportant reactions and species in a systematic, efficient and accurate manner.

1. Introduction

Detailed reaction models for C_1-C_4 hydrocarbons usually contain over 100 species in about 1000 elementary reactions [1–6]. Direct application of such models is limited only to simple, canonical combustion simulations because of their tremendous computational cost. Various reduction techniques have been developed to accommodate realistic fuel chemistry simulations, and to capture intricacies of chemical kinetics in complex multi-dimensional combustion systems. As the first step in developing model reduction, it is important to extract a subset of the detailed reaction model, *skeletal model*, by eliminating unimportant species and reactions [7,8]. Local sensitivity analysis (SA), reaction flux analysis [9–11], and directed relation graph (DRG) and its variants [12–15] have often been utilized for skeletal model reduction. Local SA, which is the subject of the present work, explores the response of model output to a small change of a parameter from its nominal value [16] while global sensitivity analysis is useful for studying uncertainty of kinetic parameters (*i.e.* collision frequencies and activation energies) which propagate through model and non-linear coupling effects [2,17–24].

Model reduction with local SA contains methods such as PCA [1,25–31], and construction of a species ranking [32]. In local SA, the sensitivities are commonly computed either by finite difference (FD) discretizations, directly solving a sensitivity equation (SE), or by an adjoint equation (AE) [33]. The computational cost of using FD or SE, which are *forward* in time methods, scales linearly with the number of parameters making them impracticable when sensitivities with respect to a large number of parameters are needed. On the other hand, computing sensitivities with AE requires a *forward-backward* workflow, but the computational cost is independent of the number of parameters as it requires solving a single ordinary/partial differential equation (ODE/PDE) [34–36]. The AE solution is tied to the objective function, and for cases where multiple objective functions are of interest, the same number of AEs must be solved. Regardless of the method of computing sensitivities, the output of FD, SE, and AE at each time instance is the full sensitivity coefficient matrix, which can be extremely large for systems with large number of parameters.

Recently, the forced optimally time dependent (f-OTD) decomposition method was introduced for computing sensitivities in evolutionary systems using a *model driven* low-rank approximation [33]. This methodology is the extension of OTD

☆ Fully documented templates are available in the elsarticle package on CTAN.

* Corresponding author.
E-mail address: arn36@pitt.edu (A.G. Nouri).

https://doi.org/10.1016/j.combustflame.2021.111684
0010-2180/

decomposition in which a mathematical framework is laid out for the extraction of the low-rank subspace associated with transient instability of the dynamical system [37]. The OTD approximates sensitivities with respect to initial conditions, while f-OTD approximates sensitivities with respect to external parameters, *e.g.*, forcing. As a consequence, in the formulation of f-OTD there is a two–way coupling between the evolution of the f-OTD modes and the f-OTD coefficients, whereas in OTD formulation, the evolution of the modes is independent of the coefficients. In *forward* workflow of f-OTD, the sensitivity matrix *i.e.* $S(t) \in \mathbb{R}^{n_{eq} \times n_r}$ is modeled on-the-fly as the multiplication of two skinny matrices $U(t) = [\boldsymbol{u}_1(t), \boldsymbol{u}_2(t), \cdots, \boldsymbol{u}_r(t)] \in \mathbb{R}^{n_{eq} \times r}$, and $Y(t) = [\boldsymbol{y}_1(t), \boldsymbol{y}_2(t), \cdots, \boldsymbol{y}_r(t)] \in \mathbb{R}^{n_r \times r}$ which contain the f-OTD modes and f-OTD coefficients, respectively, where n_{eq} is the number of equations (or outputs), n_r is the number of independent parameters, $r \ll \min\{n_s, n_r\}$ is the reduction size, and $S(t) \approx U(t)Y^T(t)$. The key characteristic of f-OTD is that both $U(t)$ and $Y(t)$ are time-dependent and they evolve based on closed form evolution equations extracted from the model, and are able to capture sudden transitions associated with the largest finite time Lyapunov exponents [38]. The time-dependent bases have also been used for stochastic reduced order modeling [39–43], and recently for on-the-fly reduced order modeling of reactive species transport equation [44]. In a nutshell, f-OTD workflow i) is *forward* in time unlike AE, ii) bypasses the computational cost of solving FD and SE, or other data-driven reduction techniques, and iii) stores the modeled sensitivities in a *compressed* format, *i.e.* we only store and solve for two skinny matrices U and Y instead of storing and solving the full sensitivity matrix S, as in FD, SE and AE.

The major advantage of PCA in skeletal reduction is to combine the sensitivity coefficients for a wide range of operating conditions (*e.g.* equivalence ratio and pressure) [1]. The PCA finds the low-dimensional subspace of data gathered from different (temporal or spatial) locations by applying a minimization algorithm over the whole data at once. Therefore, PCA is a low-rank approximation in a time-averaged sense and may fail to capture highly transient finite-time events (*e.g.* ignition). In order to resolve this issue, one needs to pre-recognize the locations of such events and use the data mainly from these locations. This requires extensive knowledge and/or expertise. Moreover, PCA modes are time invariant, and the process of selecting sufficient eigenvalues/eigenmodes to capture the essence of all observed phenomena (*e.g.* ignition, flame propagation), is crucial but is usually done by trial and error. References [1,45] show that for certain problems, a skeletal model built solely upon the information conveyed by that first reaction group (first eigenmode) from PCA can fail to accurately reproduce the detailed model over the entire domain of interest. Therefore, one needs to deal with several eigenmodes with close eigenvalues and choose essential reaction groups among them [1].

In order to resolve the drawbacks of current SA methods and PCA for skeletal model reduction, we use f-OTD methodology for both SA and skeletal model reduction. The applicability of our approach is demonstrated for ethylene-air burning with the University of Southern California (USC) chemistry model [2] as the detailed model. Adiabatic, constant pressure, spatially homogeneous ignition is the canonical problem; and the generated skeletal models with f-OTD are compared against detailed and several skeletal models.

The remainder of this paper is organized as follows. The theoretical description of PCA and f-OTD and their mathematical derivations for SA are presented in Section 2. Model reduction with f-OTD is first described in Section 3, with a simple reaction model for hydrogen-oxygen combustion, followed by skeletal model reduction with f-OTD for the more complex ethylene-air system in Section 4. The paper ends with conclusions in Section 5. All the generated models are supplied in supplementary materials section.

2. Formulation

Consider a chemical system of n_s species reacting through n_r irreversible reactions,

$$\sum_{k=1}^{n_s} \nu'_{kj} \mathbb{M}_k \rightarrow \sum_{k=1}^{n_s} \nu''_{kj} \mathbb{M}_k, \quad j = 1, \dots n_r, \tag{1}$$

where $\mathbb{M}_k$ is a symbol for species k, and ν'_{kj} and ν''_{kj} are the molar stoichiometric coefficients of species k in reaction j. Changes of mass fractions $\psi = [\psi_1, \psi_2, \dots, \psi_{n_s}]^T$ and temperature T in an adiabatic, constant pressure p, and spatially homogeneous reaction system of ideal gases can be described by the following initial value problems (IVPs) [46]

$$\frac{d\psi_k}{dt} = f_{\psi_k}(\psi, T, \alpha) = \frac{W_k}{\rho} \sum_{j=1}^{n_r} \nu_{kj} \mathcal{Q}_j, \quad \psi(0) = \psi_0, \tag{2a}$$

$$\frac{dT}{dt} = f_T(\psi, T, \alpha) = -\frac{1}{c_p} \sum_{k=1}^{n_s} h_k f_{\psi_k}, \quad T(0) = T_0, \tag{2b}$$

where $t \in [0, t_f]$ is time, t_f is the final time and W_k and h_k are the molecular weight and enthalpy of species k, respectively, and

$$\nu_{kj} = \nu''_{kj} - \nu'_{kj}, \tag{3a}$$

$$\mathcal{Q}_j = \alpha_j \mathcal{K}_j \prod_{m=1}^{n_s} \left(\frac{\rho \psi_m}{W_m} \right)^{\nu'_{mj}}. \tag{3b}$$

Here, $\alpha = [1, 1, \dots, 1] \in \mathbb{R}^{n_r}$ is the vector of perturbation parameters and $\mathcal{K}_j$ is the rate constant of reaction j which is usually modeled using the modified Arrhenius parameters [47] for elementary reactions (Note: all reversible reactions are cast as irreversible reactions). In Eq. (2) $\rho(T, \psi)$ and $c_p(T, \psi) = \sum_{k=1}^{n_s} \psi_k c_{p_k}(T)$ are the density and specific heat at constant pressure of the mixture, respectively, where $c_{p_k}(T)$ is the specific heat at constant pressure of kth species given by the NASA coefficient polynomial parameterization [48]. Let $\xi = [\psi, T] \in \mathbb{R}^{n_{eq}}$ denote the vector of compositions and accordingly $\boldsymbol{f} = [\boldsymbol{f}_{\psi}, f_T]$ where $n_{eq} = n_s + 1$. Then the compositions IVP is governed by:

$$\frac{d\xi_i}{dt} = f_i(\xi, \alpha), \quad \xi(0) = [\psi_0, T_0]. \tag{4}$$

Since $\alpha = \mathbf{1}$, the perturbation with respect to α_j amounts to an infinitesimal perturbation of progress rates $\mathcal{Q}_j$ for $j = 1, 2, \dots, n_r$. The sensitivity matrix, $S(t) = [\boldsymbol{s}_1(t), \boldsymbol{s}_2(t), \dots \boldsymbol{s}_{n_r}(t)] \in \mathbb{R}^{n_{eq} \times n_r}$, contains local sensitivity coefficients, $\boldsymbol{s}_j = \partial \boldsymbol{\xi} / \partial \alpha_j$, and it can be calculated by solving the SE,

$$\frac{dS_{ij}}{dt} = \sum_{m=1}^{n_{eq}} \frac{\partial f_i}{\partial \xi_m} \frac{\partial \xi_m}{\partial \alpha_j} + \frac{\partial f_i}{\partial \alpha_j} = \sum_{m=1}^{n_{eq}} L_{im} S_{mj} + F_{ij}, \tag{5}$$

where $L_{im} = \frac{\partial f_i}{\partial \xi_m}$ and $F_{ij} = \frac{\partial f_i}{\partial \alpha_j}$ are the Jacobian and the forcing matrices, respectively.

2.1. Principal component analysis

Principal component analysis allows the investigation of the effects of parameter perturbations on the objective function $\mathcal{G}(\boldsymbol{p})$

$$\mathcal{G}(\boldsymbol{p}) = \int_{z_1}^{z_2} \sum_{i=1}^{n_{eq}} \left[\frac{\xi_i(z, \boldsymbol{p}) - \xi_i(z, \boldsymbol{p^0})}{\xi_i(z, \boldsymbol{p^0})} \right]^2 dz, \tag{6}$$

where $\boldsymbol{p^0}$ and $\boldsymbol{p}$ are unperturbed and perturbed normalized kinetic parameters, respectively; and $p_j = \ln \alpha_j$ for $j = 1 \dots n_r$. The integrated squared deviation is investigated on the interval $[z_1, z_2]$ of the independent variable (time and/or space) [45]. It has been

shown [25] that $\mathcal{G}(\boldsymbol{p})$ can be approximated around the nominal parameter set ($\boldsymbol{p^0}$) as,

$$\mathcal{G}(\boldsymbol{p}) \approx (\Delta \boldsymbol{p})^T \mathbb{S}^T \mathbb{S} (\Delta \boldsymbol{p}), \tag{7}$$

where $\Delta \boldsymbol{p} = \boldsymbol{p} - \boldsymbol{p^0}$ and

$$\mathbb{S} = \begin{pmatrix} \approx{S}|_{z_1} \\ \approx{S}|_{z_2} \\ \cdots \\ \cdots \\ \approx{S}|_{z_m} \end{pmatrix}_{(m.n_{eq}) \times n_r}. \tag{8}$$

Here, $\approx{S}|_{z_i}$ $(i = 1, \ldots, m)$ are normalized sensitivity matrices ($\approx{S}_{ij} = \frac{\alpha_j}{\xi_i} \frac{\partial \xi_i}{\partial \alpha_j}$) on a series of m quadrature points on $[z_1, z_2]$ to approximate the integral in Eq. (6). Eigen decomposition of $\mathbb{S}^T\mathbb{S} = A\Lambda A^T$ results in:

$$\mathcal{G}(\boldsymbol{p}) \approx \left(A^T \Delta \boldsymbol{p}\right)^T \Lambda \left(A^T \Delta \boldsymbol{p}\right), \tag{9}$$

where $\Lambda = \text{diag}\ [\lambda_1, \lambda_2, \ldots \lambda_{n_r}]$ is a diagonal matrix containing eigenvalues of $\mathbb{S}^T\mathbb{S}$ (which are real and positive) in descending order ($\lambda_1 \geq \lambda_2 \geq \ldots \geq \lambda_{n_r}$), and $A = [\boldsymbol{a}_1, \boldsymbol{a}_2, \ldots \boldsymbol{a}_{n_r}]$ contains the eigenvectors of $\mathbb{S}^T\mathbb{S}$ sorted from left to right with the same order in Λ. Then PCA uses two thresholds (λ_ϵ & a_ϵ) to select first j sets of reactions ($\boldsymbol{a}_1, \boldsymbol{a}_2, \ldots, \boldsymbol{a}_j$) which satisfy $\lambda_j > \lambda_\epsilon$ condition and choose every ith reaction in each $\boldsymbol{a}_j$ set with $|a_{ij}| > a_\epsilon$ condition [1].

2.2. Sensitivity analysis with optimally time dependent modes

Like PCA, our kinetic model reduction strategy is based on selecting reactions, whose perturbations grow most intensely in the composition evolution given by Eq. (4). However, the selection of important reactions is made here based on *instantaneous* observation of *modeled* sensitivities, unlike PCA.

2.2.1. Modeling the sensitivity matrix

Imagine we perturb the composition evolution equation (Eq. (4)) by infinitesimal variations of $\alpha_j = 1$ to $\alpha_j = 1 + \delta\alpha_j$, where $\delta\alpha_j \ll 1$ for $j = 1, 2, \ldots, n_r$. In f-OTD, we factorize the sensitivity matrix $S(t)$ into a time-dependent subspace in the n_{eq}-dimensional phase space of compositions represented by a set of f-OTD modes: $U(t) = [\boldsymbol{u}_1(t), \boldsymbol{u}_2(t), \cdots, \boldsymbol{u}_r(t)] \in \mathbb{R}^{n_{eq} \times r}$. These modes are orthonormal $\boldsymbol{u}_i^T(t)\boldsymbol{u}_j(t) = \delta_{ij}$ at all t, where δ_{ij} is the Kronecker delta. The rank of $S(t) \in \mathbb{R}^{n_{eq} \times n_r}$ is $d = \min\{n_{eq}, n_r\}$ while the f-OTD modes represent a rank-r subspace, where $r \ll d$. To this end, we approximate the sensitivity matrix via the f-OTD decomposition (Fig. 1):

$$S(t) \approx U(t) Y^T(t), \tag{10}$$

where $Y(t) = [\boldsymbol{y}_1(t), \boldsymbol{y}_2(t), \cdots, \boldsymbol{y}_r(t)] \in \mathbb{R}^{n_r \times r}$ is the f-OTD coefficient matrix. The above decomposition is not exact as Eq. (10) is a low-rank approximation of the sensitivity matrix $S(t)$. Note that in the above decomposition both $U(t)$ and $Y(t)$ are time dependent. We drop the explicit time dependence on t for brevity. Fig. 1 shows the schematic of decomposition of S into f-OTD components U and Y. The evolution equation for U and Y are obtained by substituting Eq. (10) into Eq. (5):

$$\frac{dS}{dt} \approx \frac{dU}{dt} Y^T + U \frac{dY^T}{dt} = LUY^T + F. \tag{11}$$

Projecting Eq. (11) to U results in

$$U^T \frac{dU}{dt} Y^T + U^T U \frac{dY^T}{dt} = U^T LUY^T + U^T F. \tag{12}$$

The f-OTD modes are orthonormal, $U^TU = I$. Taking a time derivative of the orthonormality condition yields in: $\frac{dU^T}{dt}U + U^T\frac{dU}{dt} = 0$. This means that $\varphi = U^T \frac{dU}{dt} \in \mathbb{R}^{r \times r}$ is a skew-symmetric matrix ($\varphi^T = -\varphi$). As shown in Refs. [33,37], any skew-symmetric choice of matrix φ, will lead to equivalent f-OTD subspaces. Here we choose $\varphi = 0$. Using $U^TU = I$ and $U^T\frac{dU}{dt} = 0$, Eq. (12) simplifies to

$$\frac{dY^T}{dt} = U^T LUY^T + U^T F. \tag{13}$$

The evolution equation for U can be obtained by substituting $\frac{dY^T}{dt}$ from Eq. (13) in Eq. (11) and projecting the resulting equation onto Y by multiplying Y from right

$$\frac{dU}{dt} = QLU + QFYC^{-1}, \tag{14}$$

where $Q = I - UU^T$ is the orthogonal projection onto the space spanned by the complement of U and $C = Y^TY \in \mathbb{R}^{r \times r}$ is a *correlation matrix* matrix. Matrix $C(t)$ is, in general, a full matrix implying that the f-OTD coefficients are correlated. Eq. (13) can be written as

$$\frac{dY}{dt} = YL_r^T + F^TU, \tag{15}$$

where $L_r = U^TLU \in \mathbb{R}^{r \times r}$ is a reduced linearized operator. Eqs. (14) and (15) are a coupled system of ODEs and they constitute the f-OTD evolution equations. The f-OTD modes align themselves with the most instantaneously sensitive directions of the composition evolution equation when perturbed by α. It is shown in Ref. [38] that when α is the perturbation to the initial condition, the OTD modes converge exponentially to the eigen-directions of the CauchyGreen tensor associated with the most intense finite-time instabilities. We refer to Ref. [37] for further details about OTD.

2.2.2. Selecting important reactions & species

In our approach, instantaneous sensitivities are analyzed as opposed to PCA in which sensitivities are sampled at a few selected time instants. Computing instantaneous sensitivities would significantly increase the computational/bookkeeping costs especially if large detailed mechanisms are to be analyzed. The f-OTD leverages the fact that we are often interested in the leading sensitivity vectors, and it provides a computationally feasible approach for solving only those dominant sensitivity vectors, without requiring to explicitly compute the full sensitivities at any point. The reduction procedure is as follows:

1. Modeled sensitivities are computed in factorized format by solving Eqs. (14) and (15). These two equations are evolved in addition to Eq. (4), and the values of ξ, U, and Y are stored at resolved time steps $t_i \in [0, t_f]$. Eq. (4) is initialized with a combination of the initial temperatures, equivalence ratios (ϕ_0), *etc.* Each simulation with a different initial condition is denoted by a *case* here. Eqs. (14) and (15) are initialized by first solving the SE (Eq. (5)) for a few time steps, and then performing singular value decomposition of the sensitivity matrix $S = B\Sigma V^T$ and assigning $U = B$ and $Y = V\Sigma$.
2. At each resolved time step and for each case, we compute the eigen decomposition of $\approx{S}^T\approx{S} \in \mathbb{R}^{n_r \times n_r}$ as $\approx{S}^T\approx{S} = A\Lambda A^T$, and define $\boldsymbol{w} \in \mathbb{R}^{n_r \times 1} = (\Sigma\lambda_i|\boldsymbol{a}_i|)/(\Sigma\lambda_i) \in \mathbb{R}^{n_r}$. The $\boldsymbol{w}$ vectors are basically the average of eigenvectors of $\approx{S}^T\approx{S}$ matrix weighted based on their associated eigenvalues. This prevents us from dealing with each eigenvector ($\boldsymbol{a}_i$) separately. We use the normalized sensitivities ($\approx{S}_{ij} = \frac{\alpha_j}{\xi_i}\frac{\partial \xi_i}{\partial \alpha_j}$) of species with mass fractions greater than a threshold, *e.g.* 1.0e-6. This results in elimination of some of the rows of $\approx{S}$ associated with small mass fraction species at each time step. As shown in Sections 3 and 4, the first sorted eigenvalue (λ_1) is usually orders of magnitude larger than the

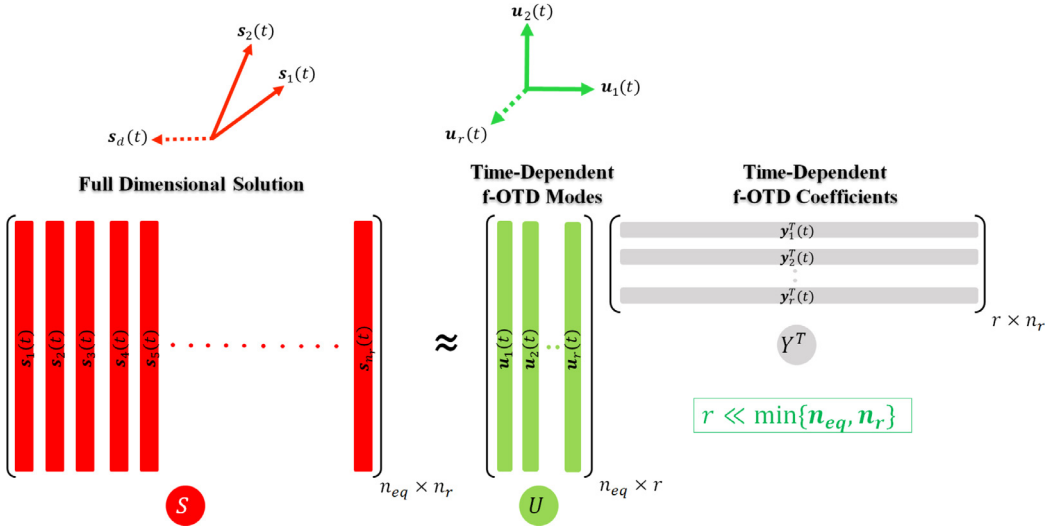

Fig. 1. Modeling sensitivity matrix $S(t)$ as a multiplication of two low-ranked matrices $U(t)$ and $Y(t)$ which evolve based on Eqs. (14) and (15).

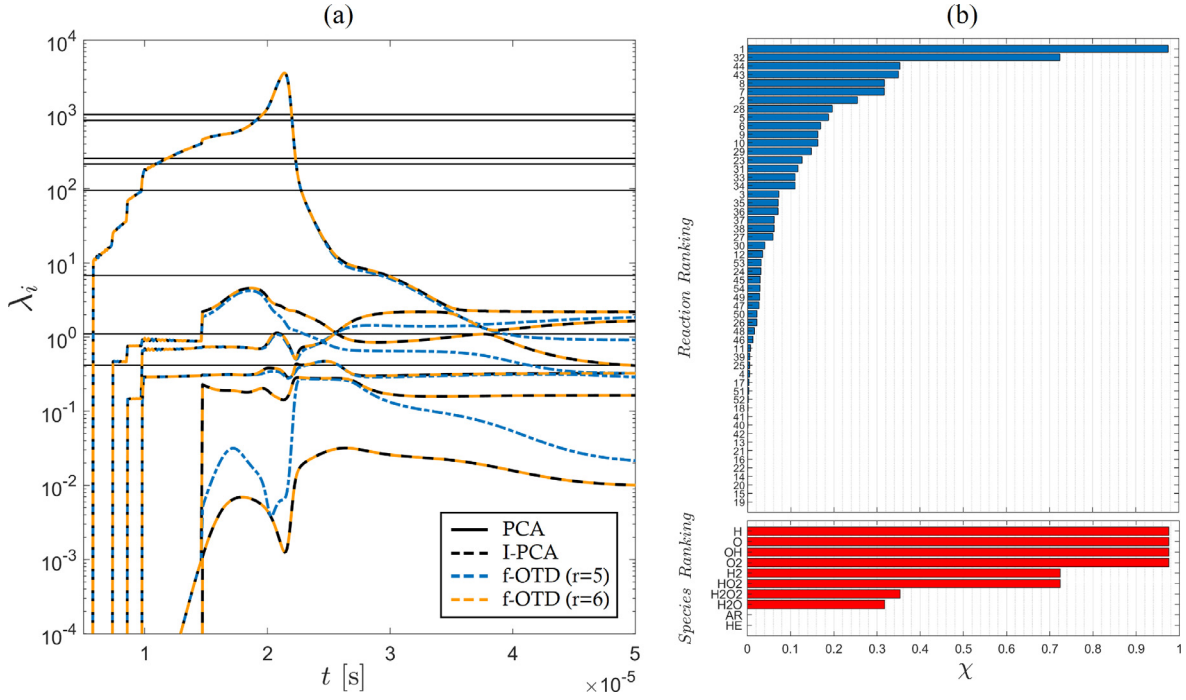

Fig. 2. Model reduction for hydrogen-oxygen: (a) eigenvalues calculated by PCA, I-PCA and f-OTD, (b) sorted reactions and species based on their associated χ values. Ignition data is gathered for stoichiometric mixture ($\phi_0 = 1.0$) at atmospheric pressure (p =1atm) with T_0=1200K.

others which means $\boldsymbol{w}(t) \approx |\boldsymbol{a}_1(t)|$. Each element of $\boldsymbol{w}$, *i.e.* w_i, is positive and associated with a certain reaction (ith reaction). The larger the w_i value, the more important reaction i is. We define χ_i as the highest value associated with w_i through all resolved time-steps and cases.

3. The elements of χ vector are sorted in descending order to find the indices of the most important reactions in the detailed model. Species are also sorted based on their first presence in the sorted reactions, *i.e.* species who first shows up in a higher ranked reaction would be more important than a species who first participate in a lower ranked reaction. This results in a reaction and species ranking based on χ vector *e.g.* Fig. 2(b).
4. In the last step, we choose a set of species by defining a threshold χ_ϵ on the element of χ vector and eliminate species whose associated χ_i are less than χ_ϵ. We also get rid of the reactions which include the species. As our skeletal model reduction is reaction based, any non-reactive species with non-zero mass fraction in the initial condition should be manually added to the skeletal model.

In summary, we sort the reactions to find the most important species. These species and the reactions which connect them together, create our reduced models. In combustion systems, perturbations with respect to "fast" reactions generate very large sensitivities for short time periods which vanish as $t \to \infty$. On the other hand, perturbations with respect to "slow" reactions generate smaller and more sustained sensitivities. As our approach is based on the instantaneous observation of sensitivities, both "slow" and "fast" reactions can leave an imprint on the instantaneous normalized reaction vector ($\boldsymbol{w}$) if their imprints are larger than the threshold value (χ_ϵ). However, if the sensitivities asso-

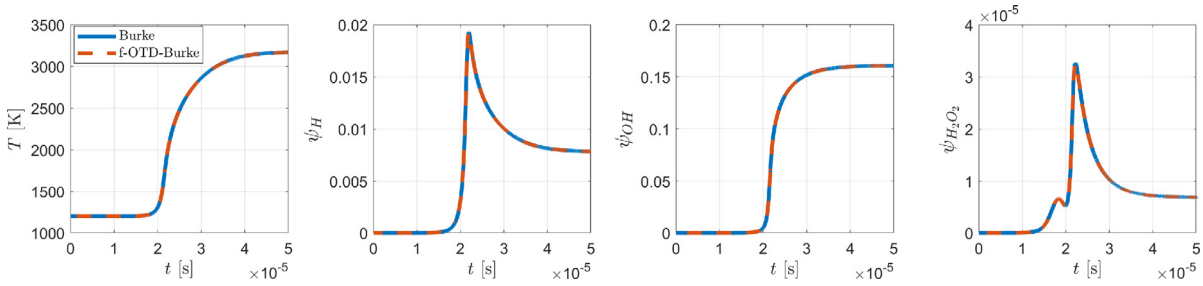

Fig. 3. Model reduction for hydrogen-oxygen: comparison of the predicted temperature and some species mass fraction profiles from different models for stoichiometric mixture ($\phi_0 = 1.0$) at atmospheric pressure (p =1atm) with T_0=1200K.

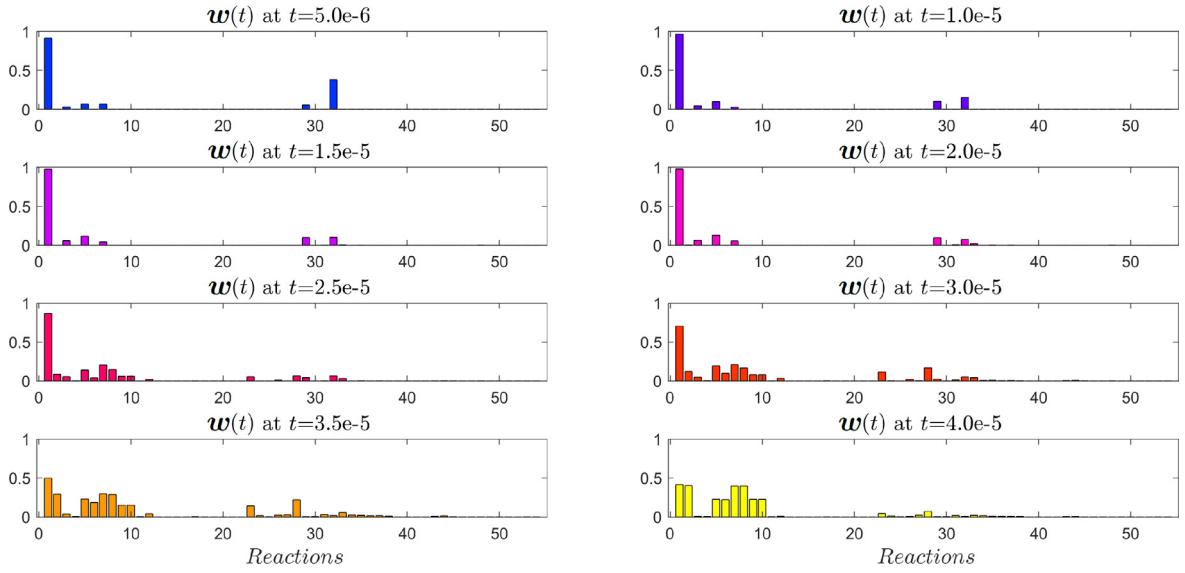

Fig. 4. Model reduction for hydrogen-oxygen: temporal variation of $w(t)$ for the ignition of a stoichiometric mixture ($\phi_0 = 1.0$) at atmospheric pressure (p =1atm) with T_0=1200K.

ciated with "fast" and "slow" reactions from all times and locations would be combined with each other before dimension reduction, as commonly done in PCA-type approaches, the smaller sensitivities associated with "slow" reactions could have been outweighted by the large sensitivities associated with "fast" reactions. In fact, this concern is the primary motivation for using f-OTD rather than PCA-type skeletal reduction approaches.

3. Model reduction with f-OTD: application for hydrogen-oxygen combustion

In this section, the process of eliminating unimportant reactions and species from a detailed kinetic model with f-OTD is described, and its differences with PCA are highlighted. The Burke model [49] for hydrogen-oxygen system which contains n_s=10 species,[1] and n_r=54 irreversible (27 reversible) reactions is considered as the detailed model. The reduction process is performed by analyzing only one case for the ignition of an adiabatic, stoichiometric hydrogen-oxygen mixture at atmospheric pressure and T_0=1200K, with integration of both the SE (Eq. (5)) and f-OTD equations (Eqs. (14) and (15)). Exact sensitivities from SE are computed for two purposes, i) finding PCA eigenmodes and eigenvalues, and ii) analyzing the performance of f-OTD by comparing the instant eigenvalues of $\tilde{\tilde{S}}^T\tilde{\tilde{S}}$ at each t, from f-OTD against those obtained by solving the SE. The latter is equivalent to performing instantaneous PCA (I-PCA) on the full sensitivity matrix. The I-PCA shows *the* optimal reduction of the time-dependent sensitivity matrix, and we show that the eigenvalues of f-OTD closely approximate the r most dominant eigenvalues of I-PCA.

Figure 2(a) compares top eigenvalues of f-OTD with PCA (static) and I-PCA (instantaneous). It is shown that the top PCA eigenvalues are time invariant, and close to each other. In contrast the first f-OTD eigenvalue is orders of magnitude larger than the others during the course of ignition, *i.e.* from t=0 to t=30 μs (until most of the heat is released). Moreover, f-OTD eigenvalues match with I-PCA with increasing number of modes (r). This means that the modeled sensitivities converge to the exact values by adding more modes, in this case addition of top 6 modes. The results also show that with f-OTD (r=5), the time variation of top eigenvalues is captured well, while the second dominant eigenvalues deviates from I-PCA solution in the main non-equilibrium reaction layer and the post heat release region. Figure 2(b) portray the reaction and species rankings for ignition problem. Note: inert species AR and HE in Fig. 2(b) are not important in pure hydrogen-oxygen ignition and can be eliminated. The f-OTD-Burke model is generated by removing these two species and their associated reactions from the Burke model with n_s=8 and n_r=46. Figure 3 demonstrates f-OTD-Burke ability in reproducing the species evolution using the Burke model, for a stoichiometric mixture ($\phi_0 = 1.0$) of hydrogen-oxygen at p=1atm and T_0=1200K. Figure 4 portrays the temporal evolution of $\boldsymbol{w}(t)$. As each element of $\boldsymbol{w}(t)$ is associated with a reaction, any change in the shape of this temporal vector signifies a change in the importance of reactions during the course of ignition. For ex-

[1] This kinetic model has 13 species (H, H_2, O, OH, H_2O, O_2, HO_2, H_2O_2, N_2, AR, HE, CO, CO_2) in which N_2, CO, and CO_2 do not participate in the reactions.

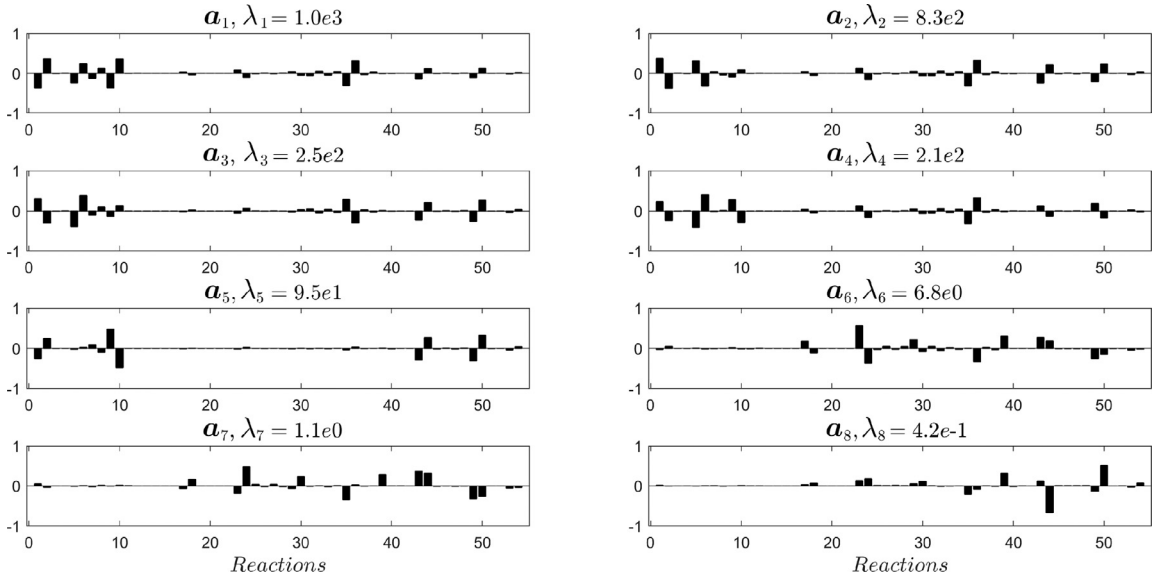

Fig. 5. Model reduction for hydrogen-oxygen: first eight eigenmodes of $\mathbb{S}^T\mathbb{S}$ calculated by PCA, from combined analysis over the time interval 0 to 5.0e-6 secs. The analysis is associated with the ignition of a stoichiometric mixture ($\phi_0 = 1.0$) at atmospheric pressure (p =1atm) with T_0=1200K.

ample the first reaction (H+O_2 → O+OH) is the most important one at t=5.0e-6, but by marching in time and passing the peak of the heat release region, other reactions (*e.g.* reactions 2–10 which are specifically radical recombination reactions like OH+OH→O+H_2O) also become important. Our model reduction approach ranks reactions based on their all time maximum value on $\boldsymbol{w}$. The f-OTD approach detects reactions even if their importance become visible instantly. Such reactions cannot be detected in static model reduction techniques such as PCA.

Figure 5 shows the first 8 eigenmodes of $\mathbb{S}^T\mathbb{S}$ matrix (Eq. (8)) and their associated eigenvalues from PCA. The parameters $\lambda_1 - \lambda_4$ have a same order of magnitudes and $\boldsymbol{a}_1 - \boldsymbol{a}_4$ introduce similar important reactions. Reactions 22 and 28 are not considered important by observing only $\boldsymbol{a}_1 - \boldsymbol{a}_4$. However, it was shown in Fig. 4 that these reactions are effective during $t \in$[3.0e-5,3.5e-5]. The next step in model reduction with PCA is to define threshold values λ_ϵ and a_ϵ to select important reactions and species as described in Section 2.1. This task is beyond the scope of this study.

4. Skeletal reduction: application for ethylene-air burning

Several detailed kinetic models for ethylene-air burning are available in literature, and are developed at the University of California, San Diego (UCSD) [4], the University of Southern California (USC - a subset of JetSurf) [2], the KAUST (AramcoMech2) [50], and the Politecnico of Milan (CRECK) [5]. Figure 6 indicates that the ignition delays as predicted by all these models are in a reasonable agreement with each other. Moreover, it is shown in Ref. [51] that USC ignition delays are closer to experimental data in comparison with the other three models. Therefore, here we consider USC as our detailed kinetic model, and extract a series of skeletal models via comparison with this baseline.

4.1. Problem setup and initial conditions

Simulations are conducted of an adiabatic, atmospheric pressure (p=1atm) reactor for 6 cases with different initial temperatures $T_0 \in$[1400,2000] and equivalence ratios $\phi \in$[0.5,1.0,1.5] for ethylene-air mixture. The USC model [2] with 111 species and 1566 irreversible (784 reversible) reactions is the detailed model based on which all the skeletal models (f-OTDs) are generated. Only three

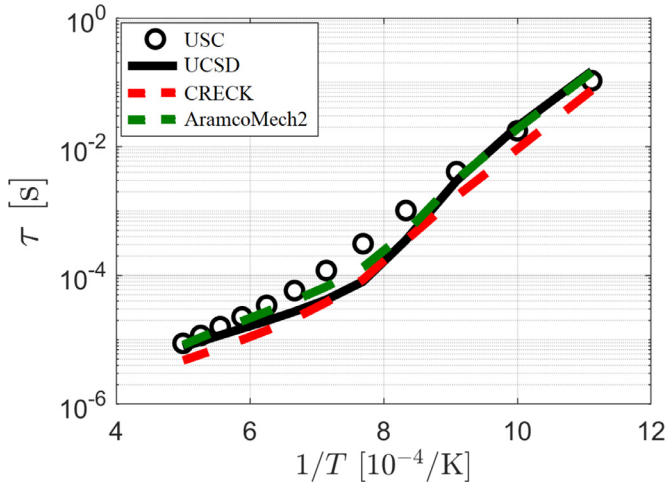

Fig. 6. Skeletal model reduction for ethylene-air: ignition delays calculated by different detailed kinetic models for an atmospheric (p=1atm) stoichiometric mixture (ϕ_0=1.0) of ethylene-air. USC, UCSD, CRECK, and AramcoMech2 are in good agreement with each other.

f-OTD modes (r=3) are employed to model the sensitivity matrix. Simulations with SK31 [1], SK32 [52] and SK38 [1], which are also skeletal models generated from two versions of USC (optimized and unoptimized), are considered. The comparisons are made based on three criteria: i) ignition delay, ii) premixed laminar flame speed, iii) non-premixed extinction strain. The flame speeds and the extinction curves are generated by Cantera [48].

4.2. Skeletal models

Figure 7(a) portrays the evolution of eigenvalues of $\tilde{\tilde{S}}^T\tilde{\tilde{S}}$ for one of the cases with T_0 =1400K and ϕ_0 =1.0. The value of $\lambda_1(t)$ is two orders of magnitude larger than $\lambda_2(t)$ during the course of ignition, except around temperature inflection point[2] (T_{inf}) in which $\lambda_1(t)$ is six orders of magnitude larger than $\lambda_2(t)$. This means that

[2] Temperature at $dT/dt|_{\max}$

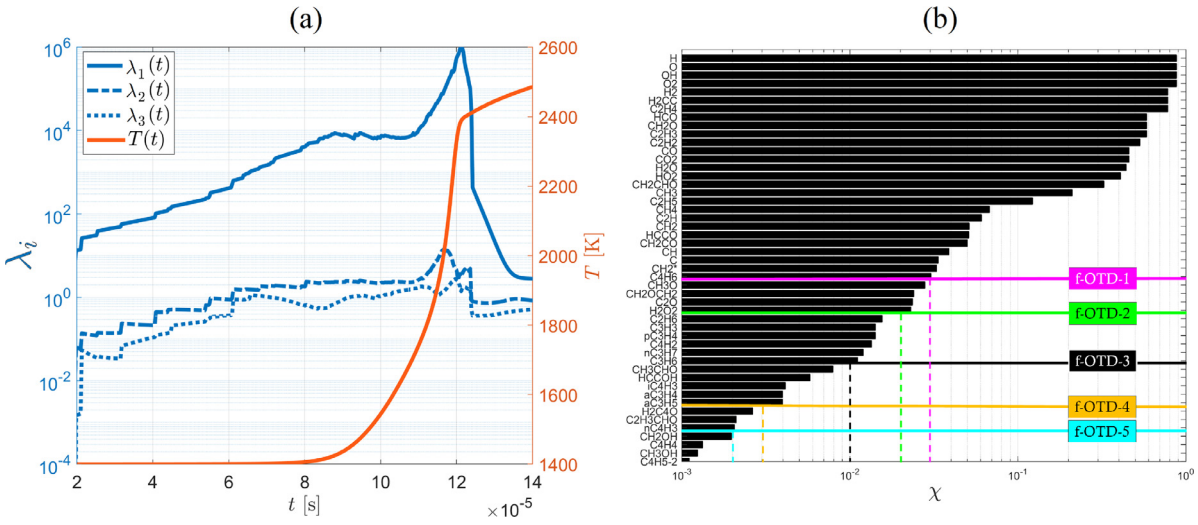

Fig. 7. Skeletal model reduction for ethylene-air: (a) eigenvalues of $\overset{\approx}{S}^T\overset{\approx}{S}$ with r=3 for ignition simulation initialized with T_0=1400K and ϕ=1.0. $\lambda_1(t)$ is orders of magnitude larger than the others during ignition. (b) Species ranking with χ_ϵ associated with f-OTD models. Only first 50 species in USC model are presented here.

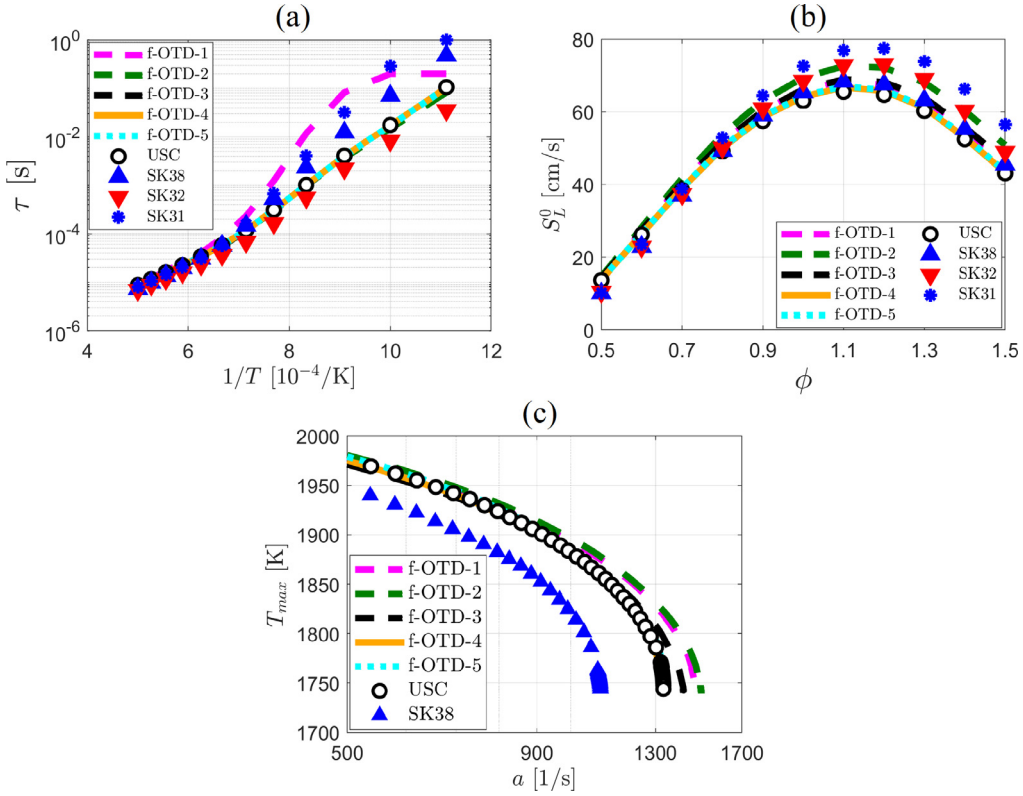

Fig. 8. Skeletal model reduction for ethylene-air: (a) predicted ignition delays, (b) flame speeds, and (c) extinction strains for skeletal models generated from USC. Ignition delays are generated with ϕ_0=1.0, flame speeds with T_0=300K, both at 1atm pressure. Extinction curves are generated for ethylene-air diffusion flame at 1atm pressure and T_0=300K.

only one of the modes of $\overset{\approx}{S}^T\overset{\approx}{S}$ is dominant during the ignition phenomenon and contains more than 95% of the energy of the dynamical system ($\lambda_1(t)/\Sigma_i\lambda_i(t) > 0.95$). Figure 7(b) shows the species ranking based on the process described in Section 2.2.2. Similar to the species ranking of hydrogen-oxygen system presented in Section 3, H, OH, O and O_2 appear as the most important species based on their associated values on χ vector for the most sensitive reaction, which is $H+O_2 \rightarrow OH+O$. Different skeletal models can be generated by putting different threshold χ_ϵ on χ and eliminating species with $\chi < \chi_\epsilon$ and their associated reactions. Our goal is to find a model which can reproduce the results of USC model based on the criteria mentioned in Section 4.1 with a pre-determined accuracy, *e.g.* less than 5% error. Table 1 provides the details of models generated with varying threshold values of χ_ϵ.

Figures 8(a) and 9(a) demonstrate that f-OTD models with $n_s \geq 32$ perfectly predict the ignition delays for the stoichiometric mixture. The SK32 model under-predicts the ignition delays while SK38 and SK31 (with slightly different rate constants from USC) over-predict the ignition delays, and the relative error associated

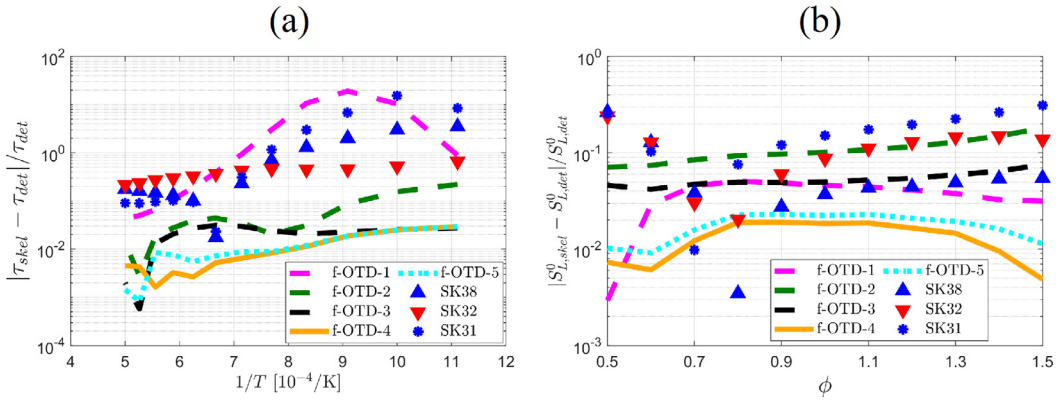

Fig. 9. Skeletal model reduction for ethylene-air: relative errors in (a) predicted ignition delays, and (b) flame speeds for skeletal models generated from USC. Ignition delays are generated with ϕ_0=1.0, flame speeds with T_0=300K, both at 1atm pressure.

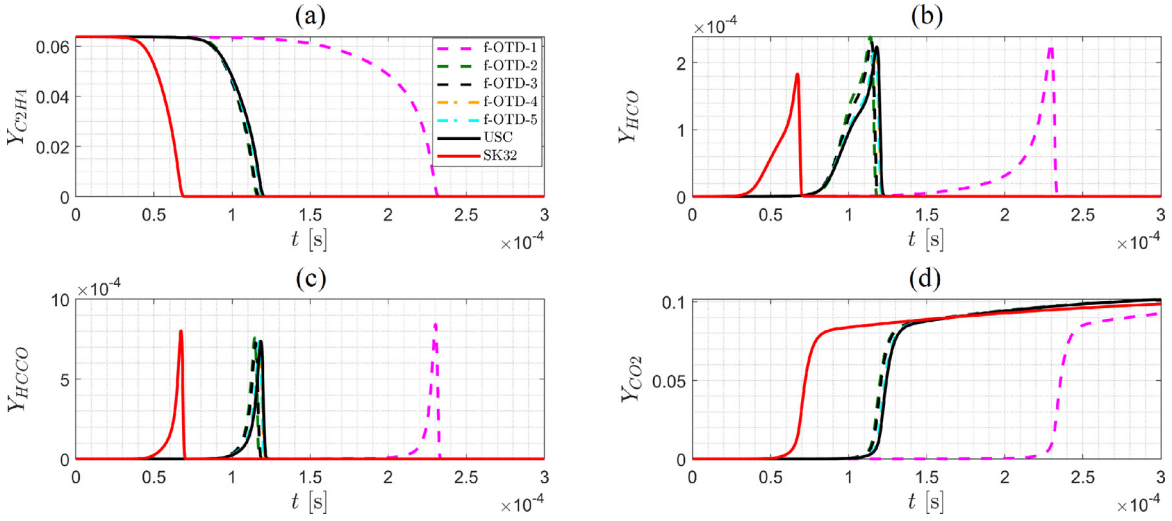

Fig. 10. Skeletal model reduction for ethylene-air: Evolution of (a) C_2H_4, (b) HCO, (c) HCCO, and (d) CO_2 mass fractions as predicted by different models in Table 1 with T_0=1400K, ϕ=1.0, and at 1atm pressure. f-OTD models with $n_s \geq 32$ show strong ability in reproducing USC results.

with these three models are usually higher than f-OTD models with $n_s \geq 32$. Figure 8(b) and 9(b) compare the laminar premixed flame speeds as predicted by different models initialized with T_0=300K. The f-OTD-2, SK31 and SK32 show largest deviations from the USC model. The f-OTD models with $n_s \geq 38$ and SK38 have the best flame speed predictions, while f-OTD models show better comparisons at lower and upper bounds of ϕ_0. Figure 8(c) compares the extinction strain rates. All f-OTD models show good agreements in estimating these rates. This is the toughest canonical flame feature to predict. The SK38 model under-predicts the maximum temperatures indicating the influence of optimized rate constants in Ref. [2].

Figure 10 portrays the species mass fraction evolution for some key species in a mixture initialized with ϕ_0=1.0 and T_0=1400K. This figure highlights the ability of f-OTD-2 (with 32 species) in predicting ignition. Moreover, all f-OTD models (with $n_s \geq 32$) provide a better estimate for the maximum mass fraction of species shown in Fig. 10 as compared with SK32 model.

Observing the results in Fig. 8, it is clear that f-OTD-1 is not a good skeletal model for USC. This is attributed to the elimination of C_2O, CH_2OCH_2, CH_3O, and H_2O_2 in this 28 species model. Although f-OTD-1 cannot predict the ignition delay accurately, it performs reasonably well in estimating laminar flame speeds and maximum temperatures for extinction. As mentioned above, f-OTD-2 estimates the ignition delays and extinction strain rate reasonably. Moreover, its flame speed predictions also match those via SK32 model. We recommend this model when 10% of relative error is tolerable in predicting ignition delays and laminar flame speeds. Predictions with f-OTD-3, f-OTD-4, and f-OTD-5 for all the test cases are so close to USC, and become more precise by increasing n_s. Comparing f-OTD-3 with f-OTD-5 based on their applications in reproducing USC model and their computational costs, we recommend the former. As Fig. 9 shows, f-OTD-3 predicts the results of USC with less than 5% relative error. Here are some differences/similarities between participating species in f-OTD models and SK32 and SK38:

Table 1
Model Characteristics.

Model	χ_ϵ	n_s	n_r
USC	–	111	1566
SK38	–	38	474
SK32	–	32	412
SK31	–	31	348
f-OTD-1	3e-2	28	324
f-OTD-2	2e-2	32	386
f-OTD-3	1e-2	38	472
f-OTD-4	3e-3	43	570
f-OTD-5	2e-3	46	610

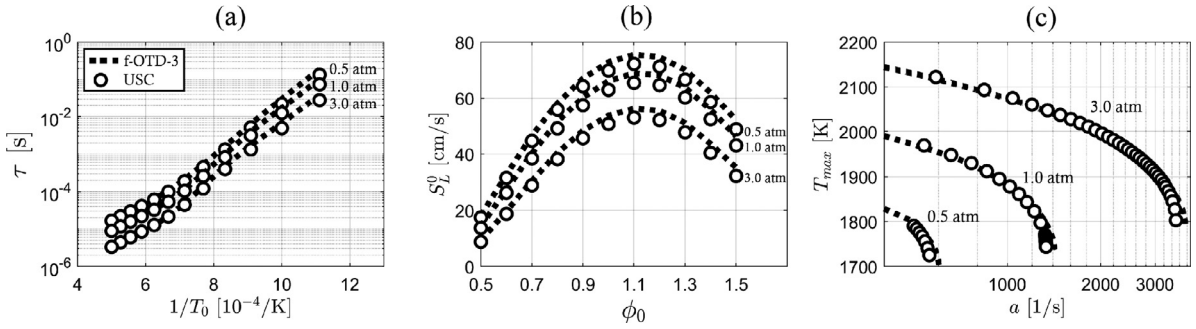

Fig. 11. Skeletal model reduction for ethylene-air: comparison of (a) ignition delay, (b) flame speed, and (c) extinction strain as predicted by the detailed model (USC) and the f-OTD-3 skeletal model. Ignition delays are generated for ϕ_0=1.0, and flame speed and extinction simulations are performed with T_0=300K.

- f-OTD-2 and SK32 (generated by DRG) both with 32 species have 27 species in common. f-OTD-2 has C, C_2H, C_2O, C_4H_6, CH_2OCH_2 but SK32 has C_2H_6, C_3H_6, CH_3CHO, aC_3H_5, nC_3H_7.
- f-OTD-3 and SK38 (generated by PCA) both with 38 species have 36 species in common. f-OTD-3 contains C_3H_3 and pC_3H_4 while SK38 has aC_3H_5 and iC_4H_3.
- f-OTD-3 has 30 species in common with SK32.

Figure 11 demonstrates the ability of f-OTD-3 in predicting ignition delay, laminar flame speed and extinction strains for three different pressures: 0.5atm, 1.0atm, and 3.0atm. f-OTD-3 shows strong ability in reproducing USC results. In this regard, it should be mentioned that the USC model contains certain reactions which are tuned for atmospheric pressure conditions. Thus, any large excursions from 1atm, *e.g.* 0.1 or 10atm, require manual selection of alternate set of rate parameters; the process we have tried to avoid here. We believe the range of pressure, *i.e.* 0.5 to 3atm (pressure ratio of 6) provides a decent test of fall-off pressure effects in our results.

4.3. Normalized or non-normalized sensitivities for f-OTD

As mentioned earlier, f-OTD analyzes the eigen decompostion of $\overset{\approx}{S}^T\overset{\approx}{S}$ instantly instead of $\mathbb{S}^T\mathbb{S}$ in PCA (Eq. 8). Using normalized sensitivities ($\overset{\approx}{S}_{ij} = \frac{\alpha_j}{\xi_i}\frac{\partial \xi_i}{\partial \alpha_j}$) can produce numerical issues where mass fractions (ξ_i) approach zero. In this study we used the normalized sensitivities of species with mass fractions greater than a threshold, *e.g.* 1.0e-6. This results in elimination of some of the rows of $\overset{\approx}{S}$ at each time step.

Another approach is to analyze the eigen decompostion of S^TS instead of $\overset{\approx}{S}^T\overset{\approx}{S}$ in f-OTD. This approach does not need a threshold for species mass fractions, and results in almost exactly the same skeletal models (f-OTD*s models). f-OTD-1*, f-OTD-3* are exactly the same as f-OTD-1 and f-OTD-3, while f-OTD-2*, f-OTD-4*, and f-OTD-5* have only one species difference with f-OTD-2, f-OTD-4, and f-OTD-5, respectively. f-OTD-2* uses C_4H_2 but f-OTD-2 uses C_2O instead, f-OTD-4* uses H_2C_4O but f-OTD-4 uses aC_3H_4 instead, and f-OTD-5* uses CH_2OH but f-OTD-5 uses C_2H_3CHO instead. Moreover, the test results do not show significant differences for this one species difference.

5. Conclusions

Instantaneous sensitivity analysis with f-OTD is described and implemented for a systematic skeletal model reduction. A key feature of the f-OTD approach is that it factorizes the sensitivity matrix into a multiplication of two low-ranked time-dependent matrices which evolve based on evolution equations derived from the governing equations of the system. Modeled sensitivities are then normalized and the most important reactions and species of a detailed model are ranked in a systematic manner based on the correlations between normalized sensitivities. It is also shown that analyzing the correlations between the non-normalized sensitivities also result in almost the same skeletal models. The significance of the f-OTD approach in model reduction is described for hydrogen-oxygen combustion, and its application for skeletal reduction is demonstrated for ethylene-air burning. The generated skeletal models are compared based on their ability to predict ignition delays, flame speeds and diffusion flame extinction strain rates. f-OTD demonstrates strong ability in eliminating unimportant species and reactions from the detailed model in an efficient manner. We recommend using f-OTD-2 and f-OTD-3 as skeletal models for USC with 10% and 5% relative errors, respectively, in estimating USC ignition delays and laminar flame speeds.

The extension of this study would include sensitivity analysis based on the most effective thermochemistry parameters *e.g.* activation energies, formation enthalpies, and transport properties *e.g.* heat and mass diffusivities. Most importantly, as shown recently [33], f-OTD can be used in solving PDEs for multi-dimensional combustion problems in a cost-effective manner — by exploiting the correlations between the spatiotemporal sensitivities of different species with respect to different parameters. This analysis can be especially insightful for problems containing rare events *e.g.* deflagration-detonation-transition by providing more insight about the global effective phenomena. Moreover, the f-OTD provides an excellent setting for development of reduced schemes in other mechanisms, for example thermonuclear reactions [53].

Declaration of Competing Interest

The authors declare that they have no known competing financial interests or personal relationships that could have appeared to influence the work reported in this paper.

Acknowledgments

This work has been co-authored by an employee of Triad National Security, LLC which operates Los Alamos National Laboratory under Contract No. 89233218CNA000001 with the U.S. Department of Energy/National Nuclear Security Administration. The work of PG was supported by Los Alamos National Laboratory, under Contract 614709. Additional support for the work at Pitt with H.B. as the PI is provided by NASA Transformational Tools and Technologies (TTT) Project Grant 80NSSC18M0150, and by NSF under Grant CBET-2042918.

Supplementary material

Supplementary material associated with this article can be found, in the online version, at doi:10.1016/j.combustflame.2021.111684.

References

[1] G. Esposito, H. Chelliah, Skeletal reaction models based on Principal component analysis: application to ethylene–air ignition, propagation, and extinction phenomena, Combust. Flame 158 (2011) 477–489.

[2] D.A. Sheen, X. You, H. Wang, T. Løvås, Spectral uncertainty quantification, propagation and optimization of a detailed kinetic model for ethylene combustion, Proc. Combust. Inst. 32 (2009) 535–542.

[3] H. Wang, E. Dames, B. Sirjean, D. Sheen, R. Tangko, A. Violi, J. Lai, F. Egolfopoulos, D. Davidson, R. Hanson, C. Bowman, C. Law, W. Tsang, N. Cernansky, D. Miller, R. Lindstedt, A High-Temperature Chemical Kinetic Model of n-Alkane (up to n-dodecane), Cyclohexane, and Methyl-, Ethyl-, n-Propyl and n-Butyl-cyclohexane Oxidation at High Temperatures (jetsurf 2.0), Tech. rep., 2011. http://melchior.usc.edu/JetSurF/JetSurF2.0.

[4] Chemical-Kinetic, Mechanisms for combustion applications," san diego mechanism web page, mechanical and aerospace engineering (combustion research), in: University of California at San Diego, http://combustion.ucsd.edu.

[5] E. Ranzi, A. Frassoldati, R. Grana, A. Cuoci, T. Faravelli, A. Kelley, C. Law, Hierarchical and comparative kinetic modeling of laminar flame speeds of hydrocarbon and oxygenated fuels, Prog. Energy Combust. Sci. 38 (2012) 468–501.

[6] C. Zhou, Y. Li, E. O'connor, K. Somers, S. Thion, C. Keesee, O. Mathieu, E. Petersen, T. De Verter, M. Oehlschlaeger, et al., A comprehensive experimental and modeling study of isobutene oxidation, Combust. Flame 167 (2016) 353–379.

[7] M.D. Smooke, Reduced Kinetic Mechanisms and Asymptotic Approximations for Methane-Air Flames: a Topical Volume, Springer, 1991.

[8] N. Peters, B. Rogg, Reduced kinetic mechanisms for applications in combustion systems, Vol. 15 of Lecture Notes in Physics, Springer-Verlag, Berlin, Germany, 1993.

[9] T. Turanyi, Reduction of large reaction mechanisms, New J. Chem. 14 (1990) 795–803.

[10] H. Wang, M. Frenklach, Detailed reduction of reaction mechanisms for flame modeling, Combust. Flame 87 (1991) 365–370.

[11] W. Sun, Z. Chen, X. Gou, Y. Ju, A path flux analysis method for the reduction of detailed chemical kinetic mechanisms, Combust. Flame 157 (2010) 1298–1307.

[12] T. Lu, C. Law, A directed relation graph method for mechanism reduction, Proc. Combust. Inst. 30 (2005) 1333–1341.

[13] X. Zheng, T. Lu, C. Law, Experimental counterflow ignition temperatures and reaction mechanisms of 1, 3-butadiene, Proc. Combust. Inst. 31 (2007) 367–375.

[14] T. Lu, C. Law, Toward accommodating realistic fuel chemistry in large-scale computations, Prog. Energy Combust. Sci. 35 (2009) 192–215.

[15] K. Niemeyer, C. Sung, M. Raju, Skeletal mechanism generation for surrogate fuels using directed relation graph with error propagation and sensitivity analysis, Combust. Flame 157 (2010) 1760–1770.

[16] S. Li, B. Yang, F. Qi, Accelerate global sensitivity analysis using artificial neural network algorithm: case studies for combustion kinetic model, Combust. Flame 168 (2016) 53–64.

[17] T. Turányi, Sensitivity analysis of complex kinetic systems, Tools Appl. J. Math. Chem. 5 (1990) 203–248.

[18] A. Saltelli, S. Tarantola, F. Campolongo, M. Ratto, Sensitivity Analysis in Practice: a Guide to Assessing Scientific Models, Vol. 1, Wiley Online Library, 2004.

[19] G. Esposito, B. Sarnacki, H. Chelliah, Uncertainty propagation of chemical kinetics parameters and binary diffusion coefficients in predicting extinction limits of hydrogen/oxygen/nitrogen non-premixed flames, Combust. Theory Model. 16 (2012) 1029–1052.

[20] I. Sobol', On sensitivity estimation for nonlinear mathematical models, Matematicheskoe modelirovanie 2 (1990) 112–118.

[21] T. Homma, A. Saltelli, Importance measures in global sensitivity analysis of nonlinear models, Reliab. Eng. Syst. Saf. 52 (1996) 1–17.

[22] H. Rabitz, O. Aliş, General foundations of high-dimensional model representations, J. Math. Chem. 25 (1999) 197–233.

[23] I. Sobol, Global sensitivity indices for nonlinear mathematical models and their monte carlo estimates, Math. Comput. Simul. 55 (2001) 271–280.

[24] G. Li, S. Wang, H. Rabitz, Practical approaches to construct RS-HDMR component functions, J. Phys. Chem. A 106 (2002) 8721–8733.

[25] S. Vajda, P. Valko, T. Turanyi, Principal component analysis of kinetic models, Int. J. Chem. Kinet. 17 (1985) 55–81.

[26] N. Brown, G. Li, M. Koszykowski, Mechanism reduction via principal component analysis, Int. J. Chem. Kinet. 29 (1997) 393–414.

[27] A. Parente, J. Sutherland, B. Dally, L. Tognotti, P. Smith, Investigation of the MILD combustion regime via principal component analysis, Proc. Combust. Inst. 33 (2011) 3333–3341.

[28] A. Parente, J. Sutherland, Principal component analysis of turbulent combustion data: data pre-processing and manifold sensitivity, Combust. Flame 160 (2013) 340–350.

[29] H. Mirgolbabaei, T. Echekki, Nonlinear reduction of combustion composition space with kernel principal component analysis, Combust. Flame 161 (2014) 118–126.

[30] A. Coussement, B. Isaac, O. Gicquel, A. Parente, Assessment of different chemistry reduction methods based on principal component analysis: comparison of the MG-PCA and score-PCA approaches, Combust. Flame 168 (2016) 83–97.

[31] M. Malik, B. Isaac, A. Coussement, P. Smith, A. Parente, Principal component analysis coupled with nonlinear regression for chemistry reduction, Combust. Flame 187 (2018) 30–41.

[32] A. Stagni, A. Frassoldati, A. Cuoci, T. Faravelli, E. Ranzi, Skeletal mechanism reduction through species-targeted sensitivity analysis, Combust. Flame 163 (2016) 382–393.

[33] M. Donello, M. Carpenter, H. Babaee, Computing sensitivities in evolutionary systems: areal-time reduced order modeling strategy, arXiv:2012.14028.

[34] K. Braman, T. Oliver, V. Raman, Adjoint-based sensitivity analysis of flames, Combust. Theory Model. 19 (2015) 29–56.

[35] M. Lemke, L. Cai, J. Reiss, H. Pitsch, J. Sesterhenn, Adjoint-based sensitivity analysis of quantities of interest of complex combustion models, Combust. Theory Model. 23 (2019) 180–196.

[36] R. Langer, J. Lotz, L. Cai, F.v. Lehn, K. Leppkes, U. Naumann, H. Pitsch, Adjoint sensitivity analysis of kinetic, thermochemical, and transport data of nitrogen and ammonia chemistry, Proc. Combust. Inst.

[37] H. Babaee, T. Sapsis, A minimization principle for the description of modes associated with finite-time instabilities, Proc. R. Soc. A 472 (2016) 20150779.

[38] H. Babaee, M. Farazmand, G. Haller, T. Sapsis, Reduced-order description of transient instabilities and computation of finite-time lyapunov exponents, Chaos 27 (2017) 063103.

[39] T. Sapsis, P. Lermusiaux, Dynamically orthogonal field equations for continuous stochastic dynamical systems, Physica D 238 (2009) 2347–2360.

[40] M. Cheng, T. Hou, Z. Zhang, A dynamically bi-orthogonal method for time-dependent stochastic partial differential equations i: derivation and algorithms, J. Comput. Phys. 242 (2013) 843–868.

[41] H. Babaee, M. Choi, T. Sapsis, G. Karniadakis, A robust bi-orthogonal/dynamically-orthogonal method using the covariance pseudo-inverse with application to stochastic flow problems, J. Comput. Phys. 344 (2017) 303–319.

[42] H. Babaee, An observation-driven time-dependent basis for a reduced description of transient stochastic systems, Proc. R. Soc. Lond. A 475 (2019) 20190506.

[43] P. Patil, H. Babaee, Real-time reduced-order modeling of stochastic partial differential equations via time-dependent subspaces, J. Comput. Phys. 415 (2020) 109511.

[44] D. Ramezanian, A. Nouri, H. Babaee, On-the-fly reduced order modeling of passive and reactive species via time-dependent manifolds, Comput. Methods Appl. Mech. Eng. 382 (2021) 113882.

[45] I. Zsély, T. Turányi, The influence of thermal coupling and diffusion on the importance of reactions: the case study of hydrogen–air combustion, Phys. Chem. Chem. Phys 5 (2003) 3622–3631.

[46] I. Zsely, J. Zador, T. Turanyi, Similarity of sensitivity functions of reaction kinetic models, J. Phys. Chem. A 107 (2003) 2216–2238.

[47] F.A. Williams, Turbulent combustion, in: J.D. Buckmaster (Ed.), The Mathematics of Combustion, SIAM, Philadelphia, PA, 1985.

[48] D. Goodwin, H. Moffat, R. Speth, Cantera: an object-oriented software toolkit for chemical kinetics, Thermodynamics, and Transport Processes, Version 2.3.0, 2017. http://www.cantera.org

[49] M. Burke, M. Chaos, Y. Ju, F. Dryer, S. Klippenstein, Comprehensive h2/o2 kinetic model for high-pressure combustion, Int. J. Chem. Kinet. 44 (2012) 444–474.

[50] C. Zhou, Y. Li, E. O'connor, K. Somers, S. Thion, C. Keesee, O. Mathieu, E. Petersen, T. De Verter, M. Oehlschlaeger, et al., A comprehensive experimental and modeling study of isobutene oxidation, Combust. Flame 167 (2016) 353–379.

[51] G. Pio, V. Palma, E. Salzano, Comparison and validation of detailed kinetic models for the oxidation of light alkenes, Ind. Eng. Chem. Res. 57 (2018) 7130–7135.

[52] Z. Luo, C. Yoo, E. Richardson, J. Chen, C. Law, T. Lu, Chemical explosive mode analysis for a turbulent lifted ethylene jet flame in highly-heated coflow, Combust. Flame 159 (2012) 265–274.

[53] A. Nouri, P. Givi, D. Livescu, Modeling and simulation of turbulent nuclear flames in type ia supernovae, Prog. Aerosp. Sci. 108 (2019) 156–179.